THE AMERICAN SOCIETY OF MECHANICAL ENGINEERS
Three Park Avenue, New York, N.Y. 10016-5990

99-GT-17



# EXPERIMENTAL MEASUREMENTS OF ACTIVELY CONTROLLED BEARING DAMPING WITH AN ELECTRORHEOLOGICAL FLUID


**John M. Vance**
Mechanical Engineering Department
Texas A & M University

**Daniel Ying**
Turbine Manufacturing Division
ABB Power Generation, Inc.

## ABSTRACT

Selection criteria and design evaluations of several types of bearing dampers with active control for application to aircraft engines were described in a companion paper (Vance, Ying, and Nikolajsen, 1999). A disk type electrorheological (ER) damper was chosen for further study and testing. The results of the tests and the final conclusions of the study are described in this paper. Experimental results including stiffness and damping coefficients are presented for the ER bearing damper with two types of ER fluid, 350 CS and 10 CS (centistokes) viscosity. The vibration attenuation performance of the ER damper was measured on a rotordynamic test rig in the form of free vibration decay, rotor orbits, and runup unbalance responses. The results show that the ER fluid with lower viscosity has the better characteristics for rotordynamic applications. It was found that ER fluids produce both Coulomb and viscous damping. If only the damping is considered, the Coulomb type is less desirable, but with active control it can also achieve control of rotor stiffness as analyzed in Vance and San Andres (1999). A feedback control system was developed and applied to the ER damper with the objective of improving the overall rotordynamic performance of the rotor bearing system, considering both vibration amplitudes and dynamic bearing forces. A "bang-bang" (on and off) simple control logic was found to work better in practice than more sophisticated schemes. The measured runup responses of the rotor-bearing system with this control approximated the desired vibration response curves fairly well. The tests highlighted some of the practical considerations that would be important for aircraft engine applications, such as the ER fluid limitations, the electrical power supply requirements, the electrical insulation requirements, the nonlinear relationship between the voltage and the damping, and the relative benefits of active control. It is concluded that active control of bearing damping is probably not a practical improvement over the passive squeeze film dampers currently used in most aircraft gas turbine engines.

## INTRODUCTION

Selection criteria and design evaluations of several types of bearing dampers with active control were described in a companion paper by Vance, Ying, and Nikolajsen (1999) for application to aircraft engines. A disk type electrorheological (ER) damper was chosen for further study and testing in a laboratory test rig (Figure 1). The results of these experiments are described in this paper.

The function of bearing dampers (or vibration dampers) in turbomachines is to reduce rotor vibration. This is normally accomplished by introducing additional damping to the bearing support. A popular device for rotor vibration control in turbomachines is the squeeze film damper (SFD). The performance of a SFD is mainly restricted by the fluid viscosity, which normally is a function of temperature. Experimental research has also shown SFD to be influenced strongly by air entrainment and air bubbles, which are difficult to predict and control.

A novel electrorheological (ER) or electroviscous (EV) damper that is easily adapted to active control was initially developed by Nikolajsen (see Nikolajsen and Hoque, 1988). Figure 2 shows a descriptive cross section. The damper contains ER fluid that thickens and provides combined Coulomb and viscous damping when an electric field is imposed across the fluid film. The ER fluid is a special fluid that has the electrorheological effect. When subjected to an electric field, typically from 500V/mm up to 6000V/mm, the fluid instantly turns from a liquid state to a gel-like solid within about 0.001 seconds. This effect increases the resistance to relative movement in the fluid. In other words, the stressed ER fluids provide more shear friction. Previous investigators including the present authors assumed that the dominant effect of the voltage would be to provide mainly a Coulomb type of damping. The rotordynamic effects of Coulomb damping are analyzed in a companion paper (Vance and San Andres, 1999). The results of the experiments to be described below will show that the damping model for a real ER fluid is actually quite complex and is yet to be precisely determined.

Presented at the International Gas Turbine & Aeroengine Congress & Exhibition
Indianapolis, Indiana — June 7–June 10, 1999
This paper has been accepted for publication in the Transactions of the ASME
Discussion of it will be accepted at ASME Headquarters until September 30, 1999

## OBJECTIVES

The objectives of this research were:

1. To experimentally explore the feasibility and performance of the ER damper at frequencies and whirl amplitudes typical of aircraft engine rotor systems.
2. To obtain experimental data that would aid optimization of the design of an ER damper for the experimental engine described in the study by Vance, Ying, and Nikolajsen (1999).
3. To develop and test a control system and software for the ER damper, and to explore the attractiveness of actively controlled dampers for possible application to turbomachinery.

These objectives were pursued by carrying out the following major tasks:

1. Modification of an existing test rig to raise the first critical speed to 6000 rpm and to improve its vibration characteristics for the purpose of identifying stiffness and damping coefficients.
2. Identification of the rotordynamic characteristics (stiffness coefficients and equivalent viscous damping coefficients) of the ER damper through experimental techniques.
3. Development of a control system for the ER damper that produces significantly better performance than the passive system.
4. Operation of the test rig to produce Bode plots (imbalance response) with and without the control system active.

## TEST RIG MODIFICATIONS

Improvement of the test rig vibration characteristics was accomplished by a redesign of the rotor system and the squirrel cage bearing support. The main problem encountered with the original rig was a low critical speed (<3000 rpm.). The modified test rig reasonably simulates the speed and vibration characteristics of a wide range of turbomachinery including aircraft engines. Figure 1 shows a sketch of the test rig after modification. The rotor operates through its first critical speed at about 5800 rpm with a light viscosity ER fluid at no voltage. A second critical speed appears around 8000 rpm as the stiffness and/or damping at the left bearing is increased by using the ER fluid. The second critical speed involves more rotor bending than the first.

The damper (Figure 2) houses five stationary plates and six whirling plates with a gap of 1.6 mm (1/16") between them. The stationary plates were assigned to a negative electrode connected to the outer squirrel-cage beams and housing. The whirling plates were selected as the positive electrode joining the inner squirrel-cage beams and whirling sleeve. The stationary plates and whirling plates were electrically insulated and sealed by a pair of non-conducting sheets. The main shaft was insulated from the damper by a plastic pipe inserted between the outer race of the bearing and the whirling sleeve. The damper housing, bearing supports and motor were seated on plastic blocks. The whole rig was electrically insulated from the base plate by applying non-conducting bushings under the tie-down bolts. In spite of all these measures taken to guarantee good electrical insulation, arcing problems persisted during the tests and the rig had to be torn down and rebuilt at one point while taking data.

Figure 1 shows three sections of the test rig. Section one on the left includes an overhung disk, an ER damper actuator, a rotating shaft and bearing supports. Section two in the middle contains a pair of bearing supports, a jackshaft and an air turbine wheel with brake disk. Section three at the right has an adjustable frequency motor (0-25000 rpm) with an accuracy of 1 rpm. The minimum controllable speed is 2000 rpm. A flexible coupling connects the main shaft and jackshaft to isolate the vibration transmitted from the motor. The air turbine is mounted on the jackshaft to help the rig start up and is also used for running speeds below 2000 rpm.

Another flexible coupling connects the jackshaft to the motor shaft. It contains a one-way clutch with maximum torque capacity of 8.3 N-m (73.6 lb-in) in one direction and with free slip in the other direction. The diameter and thickness of the overhung rotor disk are 102 mm (4.0") and 19 mm (0.75"), respectively. The length of the main shaft is 568 mm (22.37"). The bore edges of the damper housing were rounded to prevent arcing between the whirling sleeve and housing. The squirrel-cage beams are 37 mm (1.45") long with a diameter of 7.6 mm (0.3"). Nine of these beams produce the desired first critical speed. The seals used to prevent the leakage of the ER fluid are made of a 0.8 mm (1/32") thick non-conducting sheet to increase both the mechanical strength and breakdown voltage of the seal. A 4.8 mm (3/16") wide straight slot was machined into the base plate for the purpose of maintaining rotor system alignment.

## THE ER FLUID

A good ER fluid for rotordynamic application in aircraft engines should have most of the following features:

1. Chemically and physically stable, so the ER effect remains constant with time.
2. Low viscosity at zero voltage.
3. High yield shear stress with applied voltage.
4. Low conductivity and high breakdown voltage.
5. No sediment, i.e. no forced circulation of the fluid should be required.
6. High operating temperature, i.e. not a water based fluid.

Several donated samples of commercially available ER fluids were first used in the test rig without good results. Some were too viscous without voltage and some were too difficult to keep mixed. Obtaining a satisfactory ER fluid would be a major concern if the ER damper were to be adopted for operational use in aircraft engines. Two types of homemade ER fluids were found to work better in the laboratory and so were used in this research. They were formulated using cornstarch and polydimethylsiloxane fluid (silicon oil). The first one was a mixture of 350 CS liquid and corn starch in 2:1 ratio by mass. This combination was chosen for its relative chemical simplicity and its successful previous application (Stevens, et. al., 1988). The results described below from the first ER fluid (350CS) indicate that the 350CS oil was too thick for use in this application because: (1) it was difficult to pump the ER fluid into the damper housing. (2) controllability of the damping was poor, and (3) The residual viscous damping was too high (the damping values are presented later). Therefore, a second ER fluid was made by mixing 10 CS fluid with cornstarch in 4:1 ratio by mass. This fluid turned out to be much better for the purpose of these tests. Its baseline viscosity was not too high but it could still be turned solid with a high voltage. It should

be noted that these two formulations of ER fluid were used for purpose of this project only and would not have any of the other desirable operational properties listed above for aircraft engines (items 1,4,5,6).

## INSTRUMENTATION

The basic instrumentation used in the tests included a pair of proximity probes, an optical probe, a shaker system with impedance head, a synchronous tracking filter, and a dynamic signal analyzer. The proximity probes were orthogonally mounted on the housing cover to measure the relative vibration between the shaft and damper housing. Most of the vibration measurements to be described below are from these horizontal and vertical probes mounted just outboard of the bearing pedestal containing the ER damper. They will be referred as bearing #1 probes, but it is important to remember that they are actually a slight distance outboard of the bearing. An optical probe was used to measure the rotating speed of the main shaft by placing a black marker on the shaft.

The tracking filter provides both synchronous vibration amplitude (2-channel) and phase, and speed of a rotating shaft. In these experiments, the tracking filter was first used to balance the rotor and later to provide the feedback control system signal. The impedance head was used to measure driving-point frequency response of the rotor, thus identifying the damping coefficients of the ER damper. The dynamic signal analyzer has a special feature that allows transfer function curve fits for parameter identification.

The extended instrumentation included a PC computer with a 12 bit A/D board and a computer controlled high-voltage amplifier. Maximum A/D throughput depends on the operating mode and can be up to 50,000 Hz. An on-board -5 volt reference can be used to provide analog outputs in the zero to +5 VDC range, or external references (max. 10 VDC) can be used for other desired output ranges. This analog output signal was used as the control signal for the voltage applied to the damper. In this study, channel zero was used to control the high-voltage amplifier.

## THE CONTROL SYSTEM

The control system requires a high-voltage amplifier, which has unique specifications for this application. The unit is designed to allow amplification of an analog voltage in the range zero to +10 volts. The gain of this unit is set at 500, so that the maximum output is 5000 volts and 2mA. The input terminal of the unit is a 3-pin DIN socket which accepts analog voltage in the range zero to +10 volts. The input circuit is fully isolated from the high voltage output to prevent ground loops and to protect the computer from high voltage transients. There is a set of binding posts on the side of the unit, which are provided to monitor the actual high voltage output. The scale factor for this output is 0.001, meaning that a one volt signal indicates 1000 volts at the high voltage output. Although this unit is not perfect (about 350 volts offset at 60% setting.), it did provide a controllable high voltage to the ER damper. Detailed specifications of the high voltage amplifier can be found in Ying (1993). The analog output signal from the computer (which determines the voltage applied to the ER damper plates) was regulated by special software written for this application. The control algorithms will be discussed below.

## BEARING SUPPORT STIFFNESS

Static tests were performed on the rotor at each bearing of the main shaft to determine the bearing support stiffness. A force transducer was screwed onto a heavy steel block, and the block was placed under the shaft close to the bearing. A bolt was then placed between the shaft and block, one end reacting against the force transducer and the other end on the shaft. A dial gage (0.0005" resolution) was used to measure the deflection of the shaft where the force is applied. Turning the nut along the bolt varied the static force. This worked well and was repeatable for measuring the stiffness in the vertical direction. The rap tests described in a following section were used to determine the horizontal stiffness.

Figure 3 shows the static stiffness results for bearing 1 (the ER damper end). The straight line on the graph is a fit to the plot of the measured data (also shown on the graph). The same test procedure was performed for bearing 2 (coupling side). The uncertainty of this data is unknown, but the stiffness values agree well with those obtained from independent rap tests. The overall average stiffness of each bearing was obtained by averaging several static test results. The values were found to be $1.6 \times 10^6$ N/m (9148 lb/in) for bearing 1 and $26.3 \times 10^6$ N/m (150,276 lb/in) for bearing 2. The rap test results presented below show that the horizontal and vertical stiffness values are closely similar.

## FREE VIBRATION MEASUREMENTS

Rap tests (response to impact) were performed on the rotor to get the free vibration frequencies and logarithmic decrements in the time domain. Rap tests give satisfactory results for lightly damped mechanical systems with widely separated modes, but heavily damped mechanical systems with closely spaced modes create problems for the test. Ying (1993) shows how the ER damping changes the mode shapes of the test rig.

With light damping the first mode of the test rig has only a small amount of shaft bending, due to the soft bearing support. In that case most of the relative displacement is at the support containing the damper. The rap tests with no ER fluid revealed a natural frequency of 101 Hz in the horizontal direction (X probe) and 102.5Hz in the vertical direction (Y probe). The time trace showed that the vertical direction (Y) had a smaller damping ratio than that 'of the horizontal direction (X). A frequency spectrum of the rap test, from the horizontal probe at bearing 1 with no ER fluid, is shown in Figure 4. Note that there are two close peaks, 101Hz and 120 Hz, respectively. The damping in this case was light, around six percent of the critical value for the system. The critical damping ratio was calculated by using the logarithmic decrements of the time trace where the first mode is the dominant frequency (see Ying, 1993). Selecting optimum impact locations to excite the desired modes can vary modal participation in rap tests. The critical damping ratio with no ER fluid was around 6% and 4% for the horizontal direction (X) and the vertical direction (Y), respectively.

The same rap tests were performed with zero to 2500 V applied to the ER damper, filled with the 350CS

fluid. The rap test spectrum with no voltage applied to the fluid is shown in Figure 5. Two dominant peaks now appear in the rap test frequency spectrum of the damper with the ER fluid. This fluid is so viscous that it constrains the motion at the bearings, makes the bending mode more dominant, and raises its frequency. These effects become even more pronounced when voltage is applied. The time traces in these cases do not exhibit a pure frequency, so the logarithmic decrement is difficult to accurately determine. The damping is estimated from to be between 13% and 25% of the critical value, with high uncertainties.

The rap tests were repeated for the 10 CS ER fluid. The damper had to be reassembled for changing the fluid. It was difficult to keep the same damper assembly conditions, e.g. tightness of the squirrel-cage beams, for every re-assembly. Therefore, the natural frequency without the ER fluid was slightly different after re-assembly but the damping was still about six percent of the critical value. A free vibration decay trace with 10 CS fluid and with applied voltage of 500 V is shown in Figure 6. The first mode is seen to be dominant here. The percentage of critical damping is shown on the plot. Raising the voltage by a factor of five (to 2500 V) raises the damping ratio about 20%. Comparison of of the rap test results at zero voltage showed that the 350 CS fluid provided much more damping than the 10 CS fluid because of the baseline fluid viscosity. This turns out to be a very important factor when developing an active control scheme. The 10 CS fluid is to be preferred. (See Vance and San Andres, 1999, for some analytical insight).

Not shown here are the measured differences between the horizontal and vertical free vibration responses with the 10 CS fluid. They show an exponential decay in the horizontal direction (X probe) and a linear decay in the vertical direction (Y probe). The linear decay indicates that the system contains Coulomb damping (Thomson, 1993). It is unknown why the horizontal direction did not reflect a strong Coulomb damping effect. It is clear, however, that the ER fluid provides both viscous and Coulomb damping to the system.

It was also noted that the linear decays in the vertical direction appeared only for the first three peaks. The decay was exponential after the third peak. This suggests that the 10 CS fluid produced Coulomb damping for large displacements and viscous damping for small displacements in the vertical direction. For the Coulomb case (linear decay) an equivalent viscous damping coefficient and damping ratio can be calculated from the free vibration measurements. They are a function of the exciting frequency and response amplitude. These coefficients alone cannot limit the amplitude of unbalance response at the critical speed. Vance and San Andres (1999) discuss proper use of these coefficients.

## EFFECT OF THE ER DAMPER ON THE IMBALANCE RESPONSE OF THE TEST RIG

Runup imbalance responses and whirl orbits were measured on the test rig at the damper location. These tests show how the ER damper affected the rotordynamic performance of the test rig. The test consists of two parts: 1) the response without the ER fluid, and 2) the response with the ER fluid while applying various voltage levels. With no ER fluid, the maximum whirling amplitude occurred at 6000 rpm, which indicates that the baseline first critical speed is 6000 rpm (100 Hz). All the responses were synchronous with shaft speed.

The orbits of the rotor at 6000 rpm with and without ER fluid (350 CS fluid) are seen at the top of Figure 7. The whirling amplitude at the first critical speed is reduced from a maximum of 0.3 mm (12 mils) p-p (empty damper) to 0.06 mm (2.3 mils) p-p (0 volts with 350 CS ER fluid). The effect of the applied voltage from zero to 2500 volts is relatively small. The bottom of Figure 7 zooms the inside portion of the orbits to show how they change with applied voltage. It is seen that 500 volts reduces the whirling amplitude down to 0.05 mm (2.1 mils) p-p, but the applied voltage does not reduce the whirling amplitude any more. The higher applied voltage only changes the shape of the orbit. There is no distinction of the orbits for applied voltages above 1500 volts. This indicates that there is a value of optimum damping that has been exceeded with the 350 CS fluid.

The optimum damping minimizes the whirling amplitude at the critical speed. Since the ER fluid reduces the critical speed amplitudes, and since it is known that purely Coulomb damping cannot do this (Vance and San Andres, 1999), it is clear that the ER fluid produces a considerable amount of damping that is not of the Coulomb type. This non-Coulomb damping is seen here to increase with applied voltage.

The orbits are also recorded at the second critical speed (8000 rpm) and shown in Figure 8 for various applied voltages. It can be seen that the higher the applied voltage, the larger the whirling amplitude. The inereased damping (or friction) of the 350 CS ER fluid with voltage is constraining the bearing support and causing the rotor to bend more, thus increasing the response of the second mode.

Figure 9 shows the orbits with various applied voltages for the 10CS fluid at 5800 rpm (first critical speed). The whirling amplitude reduces from 0.19 mm (7.5 mils) p-p at 0 volt. down to 0.10 mm (4.1mils) p-p at 2500 volt. This figure shows that, with the 10CS fluid, the higher the applied voltage the smaller the whirling amplitude. The maximum whirling amplitude is reduced about 45% at 2500 volts compared to the zero volt amplitude. At the second critical speed (8000 rpm), the 10 CS fluid with no voltage does not increase the amplitude, but does increase it up to 80% higher than the baseline as the electric potential is raised to 2500 volts and the rotor is forced to bend in the second mode.

The orbits provide information only at a particular speed. The overall amplitude response for the entire operating speed range is shown in the rotor imbalance response curve, or the so-called Bode plot. Figure 10 shows a family of Bode plots, taken from the horizontal probe at bearing 1, with various applied voltages using 350CS ER fluid at speeds ranging from 1000 rpm to 9500 rpm. The first critical speed is 6000 rpm, which corresponds to the first peak. The 350CS ER fluid with increasing voltage suppresses vibration through the first critical speed and magnifies the vibration above the first critical speed.

The same runup tests were performed with the 10 CS ER fluid. It should be noted that the reassembled damper had a slightly different first natural frequency and modal

damping with no fluid. Figure 11 shows all the imbalance responses in the X direction for different applied voltages. The peak amplitudes at the first critical speed decrease with the increasing applied voltage, but the vibration amplitudes around the second mode increase slightly with increasing applied voltage. It was found that the first critical speed (peak location) was increased by 400 rpm in the X direction and by 200 rpm in the Y direction, respectively, while increasing the applied voltage from 0 to 2500 volts. Comparing the runup imbalance responses with the two fluids without active control, one can say that the 10CS ER fluid is to be preferred in this test rig. Clearly, there is an optimum formulation of the ER fluid for a given application that has the best characteristics of both effective damping and effective stiffness.

Figures 10 and 11 were used later to help determine the best "ON" and "OFF" speeds of the bang-bang control logic for the control system. This is discussed in a following section.

## BEARING LOADS

Two potential benefits of using variable rate dampers in aircraft turbine engines are 1) the avoidance of rubs between the rotor and stator near the critical speeds and 2) a reduction of the dynamic bearing loads for supercritical operations. Benefit 2 is illustrated in Figure 12, the bearing force transmissibility plot for three values of viscous damping [Vance, 1988]. High bearing support damping decreases the imbalance response of the rotor at the first critical speed and reduces the dynamic load transmitted through the bearing at the critical and lower speeds. But for high operating speeds, bearing support damping should be as low as possible in order to reduce the dynamic bearing loads. The bearing loads with the 10 CS fluid were calculated at applied voltages of zero and 2500 V, respectively, using the identified bearing stiffness and damping coefficients at various speeds. The bearing loads corresponding to 2500 V were found to be higher than those with zero voltage at speeds only slightly above the first critical speed, as shown in Figure 13. This suggests that zero voltage (i.e. low damping) should be applied to minimize the dynamic bearing load at these speeds. This was one of the factors influencing development of the active control logic.

## IMPEDANCE MEASUREMENTS AND CURVE FITTING

Frequency response transfer functions (FRF) were measured with the impedance head and curve-fitted to determine the undamped natural frequency and the critical damping ratio of the rotor-bearing system. The shaker was attached to the overhung disk and suspended by a pair of long rubber ropes. The shaker power amplifier was excited by random noise (frequency range from 50Hz to 450Hz). The excitation force and response acceleration signals were fed into the signal analyzer. The power amplifier was manually adjusted so as to maintain the response amplitude around .025 mm (1.0 mil) p-p. The driving-point transfer functions were averaged 100 times. The frequency response functions in the range of 50Hz to 200Hz were chosen for display and curve fitting. The signal analyzer listed the corresponding poles and zeros in a "fit table". The user should be able to judge the selection of the pole(s) of interest based on experience or some other available information (e.g. runup results). This is not difficult to do for a lightly damped linear system with distinct and dominant peaks in the frequency spectrum. This system, however, was heavily damped with closely spaced resonances and the damping is not purely viscous. The results of this procedure therefore have a high uncertainty, probably in the range of ± 50%. The amplitude of the frequency response function at the undamped natural frequency was read from the FRF and the damping coefficient was computed as $C = \omega_n/FRF$. The resulting damping coefficients with the 10 CS fluid are presented in Table 1.

## CONTROL SCHEMES IMPLEMENTED FOR THE ER DAMPER

One of the incentives to test the ER damper was to verify its suitability for a feedback control system. The control system consists of two parts. One is the control system hardware, which includes the damper actuator, probes, measuring instruments, computer, A/D board and high-voltage amplifier. The other is the software, i.e. the digitized control law. The project sponsor proposed the first version of control logic. After discussions with the authors and several iterations, a final version of this control law was ready to try with the hardware. The basic concept of this control logic was to repeatedly compare the measured vibration with a predetermined reference level and vary the ER voltage to keep the rotor vibration level as close as possible to the reference without exceeding it. This control logic would minimize the bearing loads whenever the vibration level is below the reference level because the ER damper would be turned off. Although this appeared perfect on paper, numerous problems appeared when putting it into practice. There were some constants in the code that had to be determined by experiment, which turned out to be quite difficult. Some other "fatal" errors were detected while testing the code (e.g. dead loop in comparing measured vibration level with a predetermined reference level). In order to move the project along, a much simpler "ON" and "OFF" control logic (sometimes called a bang-bang control system) was developed. This logic uses vibration only or speed only or both vibration and speed as a reference to determine the desired state. It was found that choosing speed only as a "ON" and "OFF" reference was better than the others since the amplitude versus speed characteristic of the system was well known. The bang-bang control worked so well and was so simple that the initial logic was abandoned.

Studying Figure 10 for the 350 CS fluid, one could see that the damper should be turned "ON" when the speed reaches 5400 rpm and turned "OFF" when the speed passes 7100 rpm. The "ON" condition means the applied voltage is not zero. The outline of the overlapped area on Figure 10 (the envelope under all the curves after discounting the curve with no fluid) is the expected imbalance response which has minimum vibration for the entire speed range of 1000 rpm to 9500 rpm. The voltage applied in the "ON" condition with 350 CS fluid was chosen to be 1000 V because it gives a vibration level very close to minimum with just a moderate amount of applied voltage (saving power consumption). The "OFF" condition is supposed to be zero volts. But the high

voltage power supply used in this research has about 350 volt DC offset at zero input. Therefore, it made the actual controlled imbalance response, shown in Figure 14, shift a little from the expected imbalance response. The dotted lines are the expected response and the solid lines are the measured runup imbalance responses using 350CS ER fluid incorporated with the control system.

The same procedure implemented with the 10 CS fluid yielded the runup response shown in Figure 15. In this case 2500 volts was applied between 3800 rpm and 6800 rpm. There is more discrepancy here between the expected and actual curves because electrical arcing problems required the test rig to be disassembled and rebuilt immediately after the uncontrolled tests.

This actively controlled damper does not produce the same kind of damper forces as the on-off control scheme modeled by Vance and San Andres (1999) because it turns out that ER damping is not purely Coulomb as had been earlier assumed. Nevertheless, it can be seen that the bang-bang control logic does produce results similar to the response predicted in that reference. It is simple, feasible, and works well to minimize the vibration amplitude response at the first critical speed and to minimize the dynamic bearing loads at higher speeds.

## CONCLUSIONS

1. A rotordynamic test rig was designed and constructed with an ER bearing damper that could be actively controlled by varying the voltage applied to the ER fluid.
2. Suitable ER fluids were not found to be commercially available (after considerable effort), neither for a bearing damper in aircraft engines nor for the conditions of the laboratory test rig. Fluids suitable for laboratory testing were concocted in the laboratory. Two fluids were concocted and used, with zero voltage viscosity of 10 CS and 350 CS.
3. The lower viscosity fluid was found to work better in the test rig because it amplified the second critical speed much less than the higher viscosity fluid, even at zero voltage. This finding would be generally true for rotor bending modes in aircraft engines as well because of their lightweight flexible structures (although the viscosity values could change with the application).
4. The ER fluids tested showed free vibration characteristics indicating Coulomb damping under some conditions and viscous under other conditions. The measured attenuation of critical speed peaks with increasing voltages indicates that there is a substantial amount of truly viscous damping produced by the ER damper. The type of damping observed could not be predicted *a priori*.
5. Equivalent viscous damping coefficients were measured using impedance transfer function methods, but the value uncertainty is large due to closely spaced resonances and the fact that the ER damping is not purely viscous.
6. An on-off (bang-bang) control logic was developed and implemented to actively control the bearing damping in the test rig. It proved to be successful, to the point of discouraging efforts to prove out a more sophisticated scheme.
7. The system tested was the best and most cost effective that could be identified in an extensive paper study by Vance, Ying, and Nikolajsen (1999). But the experiments reported here exposed practical problems with electrical arcing, poor availability of proper ER fluids, and the required physical size and weight of the ER damper. They all combine to raise serious questions as to whether this system could really be superior to the passive squeeze film damper as currently used in most aircraft engines.

## ACKNOWLEDGEMENT

These experiments were sponsored at Texas A&M University by the General Electric Co. under the capable direction of Mr. Al Storace. His contributions to this work are gratefully acknowledged.

## REFERENCES

Nikolajsen J.L., and Hoque, M.S. 1988, "An Electroviscous Damper", NASA CP 3026, Rotordynamic Instability Problems in High-Performance Turbomachinery, pp. 133-141.

Stevens, N.G.; Sproston, J.L. and Stanway, R., 1988, "Experimental Study of Electrorheological Torque Transmission", *Journal of Mechanisms, Transmissions, and Automation in Design*, Vol. 110, No. 2, June, pp.182-188.

Thomson, W.T., 1993, *Theory of Vibrations With Applications*, 4th Edition, Prentice Hall, , pp. 35-36.

Vance, J.M., 1988, *Rotordynamics of Turbomachinery*, John Wiley & Sons, Chapter 1.

Vance and San Andres, 1999, "Analysis of Actively Controlled Coulomb Damping for Rotating Machinery", presented at the ASME Turbo-Expo '99 Conference, Indianapolis, Indiana.

Vance, J.M., Ying, D.Z., and Nikolajsen, J.N., 1999, "Active Control Of Bearing Damping for Aircraft Engine Applications", presented at the ASME Turbo-Expo '99 Conference, Indianapolis, Indiana.

Ying, D.Z., 1993, *Experimental Study of an Electrorheological Bearing Damper With a Parametric Control System*, Master of Science Thesis, Mechanical Engineering, Texas A&M University, May.

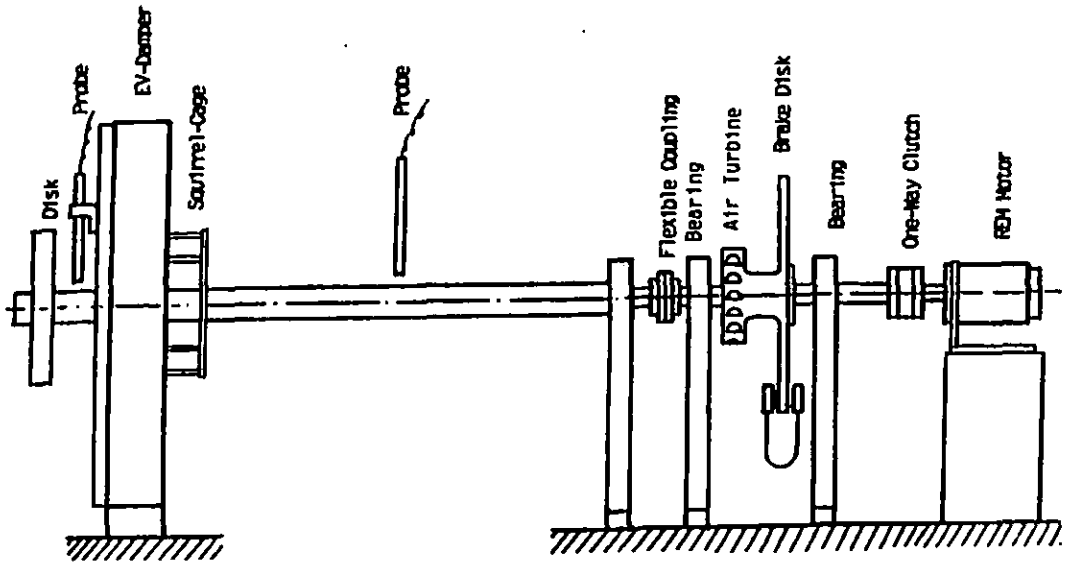


**Figure 1: Rotordynamic test rig for the ER damper**

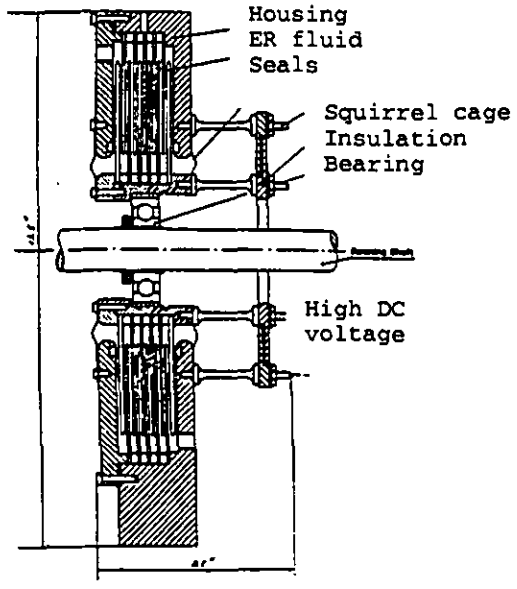


**Figure 2: Cross section of the ER damper**

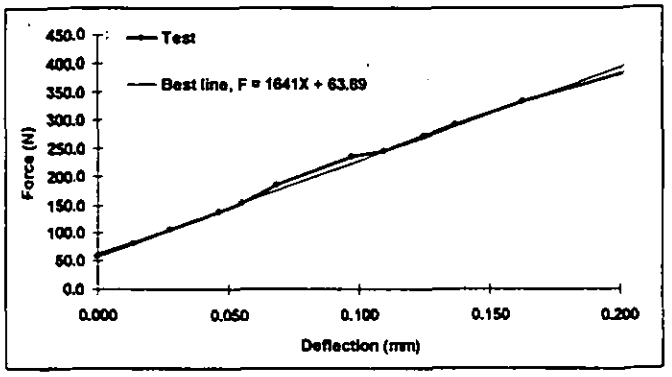


**Figure 3: Curve fit for bearing #1 stiffness**

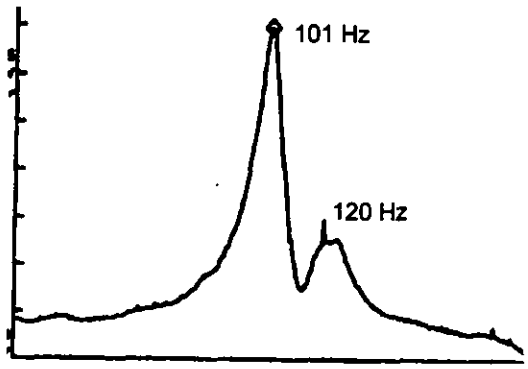


Figure 4: Rap test spectrum, X, no ER fluid

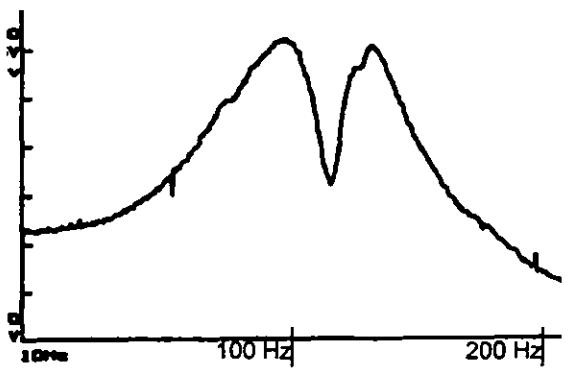


Figure 5: Rap test spectrum, X, 350 CS fluid, no voltage

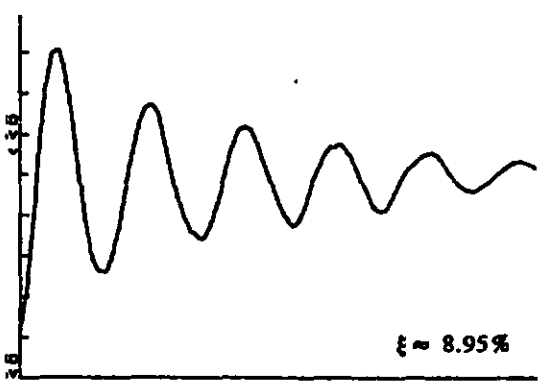


Figure 6: Time trace, 10 CS fluid, 500 V

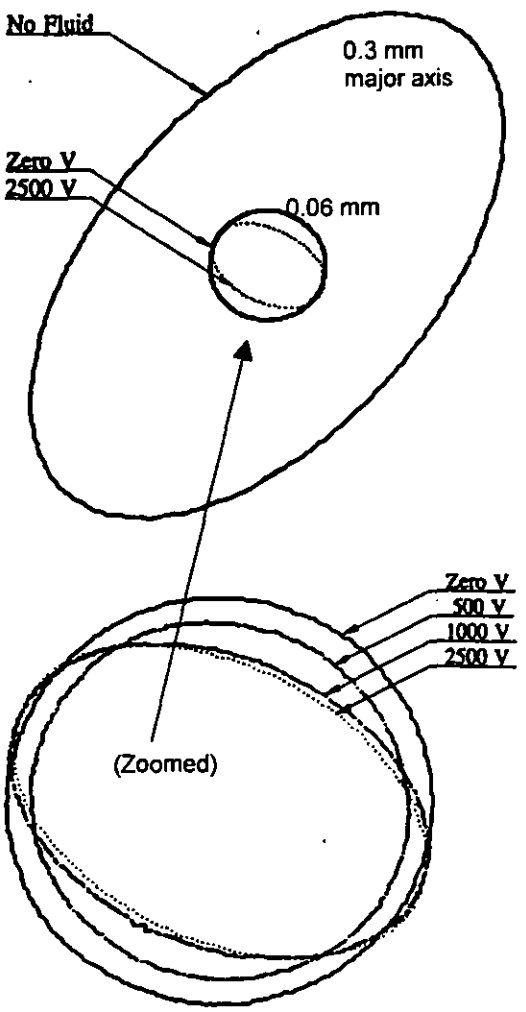


Figure 7: Rotor orbits at the first critical speed with the 350 CS fluid

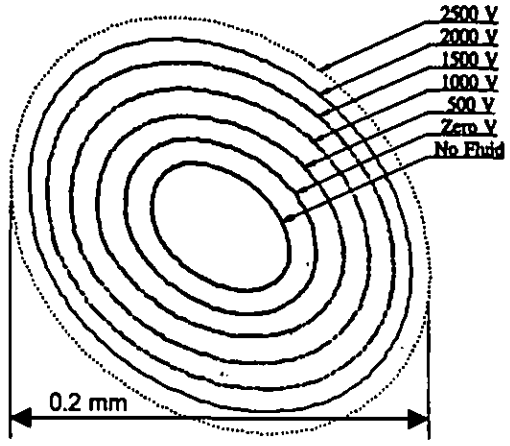


**Figure 8: Orbits at the second critical speed with the 350 CS fluid**

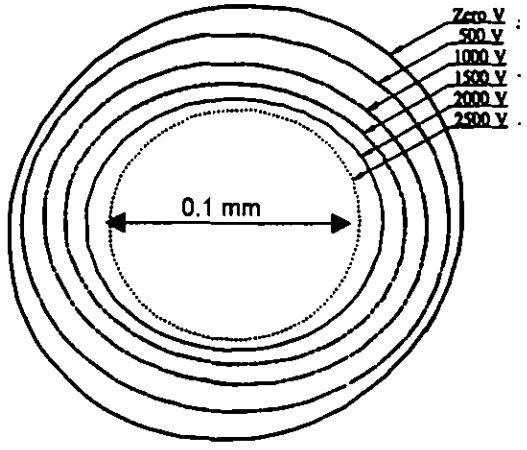


**Figure 9: Orbits at the first critical speed with the 10 CS fluid**

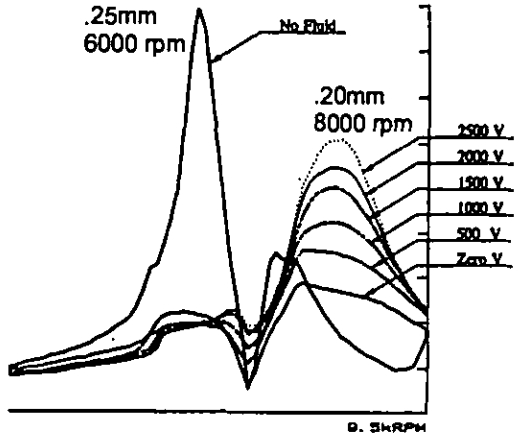


**Figure 10: Measured Bode plots with 350 CS fluid (X)**

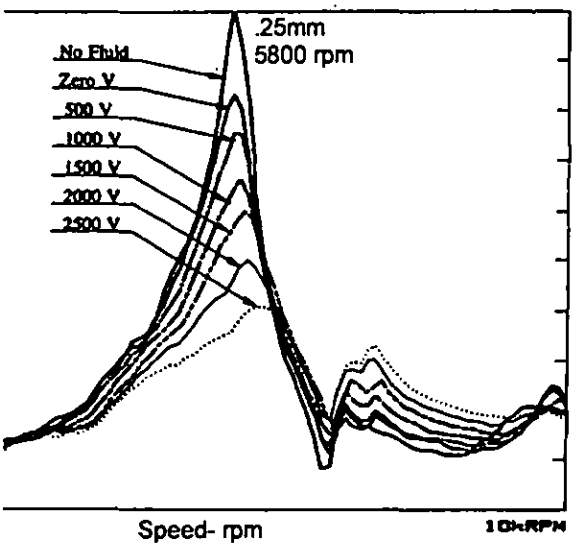


**Figure 11: Measured Bode plots with 10 CS fluid (X)**

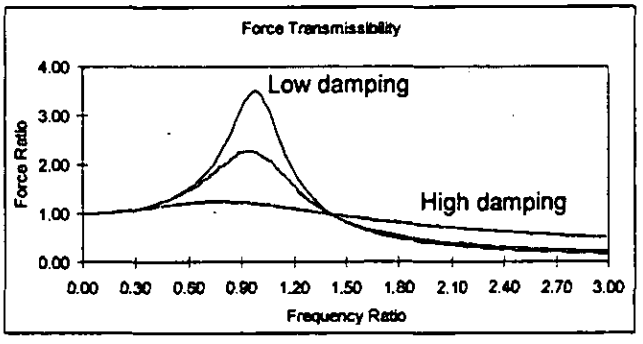


**Figure 12: Theoretical dimensionless bearing force vs. frequency ratio for three damping ratios**

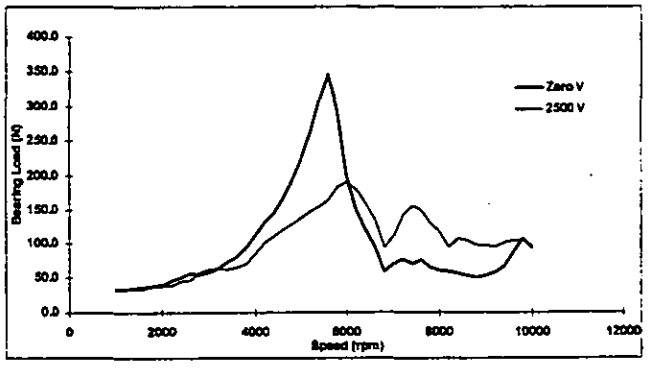


**Figure 13: Dynamic bearing loads calculated from the measured stiffness and damping coefficients, 10 CS fluid**

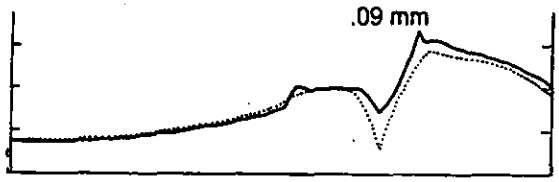


**Figure 14: Measured runup response with 350CS fluid and the control system (solid line) Dashed line is expected**

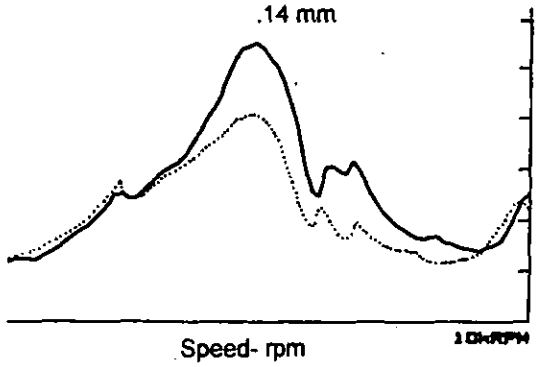


**Figure 15: Measured runup response with 10CS fluid and the control system (solid line) Dashed line is expected**

Table 1: Identified Damping Coefficients, 10 CS fluid

| | No fluid | 0 volts | 500 v | 1000 v | 1500 v | 2000 v | 2500 v |
|---|---|---|---|---|---|---|---|
| Cxx N-s/m (lb-s/in) | 560 (3.2) | 963 (5.5) | 1191 (6.8) | 1366 (7.8) | 1226 (7.0) | 1243 (7.1) | 1348 (7.7) |
| Cyy N-s/m (lb-s/in) | 473 (2.7) | 1068 (6.1) | 1488 (8.5) | 1453 (8.3) | 1173 (6.7) | 981 (5.6) | 805 (4.6) |